nature structural & molecular biology

Involvement of a chromatin remodeling complex in damage tolerance during DNA replication

Karina B Falbo[1,7], Constance Alabert[2,7], Yuki Katou[3,7], Su Wu[4], Junhong Han[5], Tammy Wehr[1], Jing Xiao[1], Xiangwei He[6], Zhiguo Zhang[5], Yang Shi[4], Katsu Shirahige[3], Philippe Pasero[2] & Xuetong Shen[1]

ATP-dependent chromatin remodeling complexes have been shown to participate in DNA replication in addition to transcription and DNA repair. However, the mechanisms of their involvement in DNA replication remain unclear. Here, we reveal a specific function of the yeast INO80 chromatin remodeling complex in the DNA damage tolerance pathways. Whereas INO80 is necessary for the resumption of replication at forks stalled by methyl methane sulfonate (MMS), it is not required for replication fork collapse after treatment with hydroxyurea (HU). Mechanistically, INO80 regulates DNA damage tolerance during replication through modulation of PCNA (proliferating cell nuclear antigen) ubiquitination and Rad51-mediated processing of recombination intermediates at impeded replication forks. Our findings establish a mechanistic link between INO80 and DNA damage tolerance pathways, indicating that chromatin remodeling is important for accurate DNA replication.

The eukaryotic genome is packaged into chromatin, which limits access to DNA for factors involved in nuclear processes such as DNA replication[1]. One prominent mechanism of chromatin modification, ATP-dependent remodeling, has been shown to regulate access to the chromatin. Moreover, the INO80 chromatin remodeling complex has been implicated in replication-related activities[2–4]. The INO80 complex is an evolutionarily conserved ATP-dependent chromatin remodeling complex that was initially described as being involved in transcription[5] and DNA repair[6–8]. However, recent evidence suggests that INO80 is important for the replication of late-firing origins of replication under stress[2] as well as for the progression of replication forks after release from HU-induced S-phase arrest[3,4]. Nonetheless, mechanistic links between chromatin remodeling and DNA replication remain poorly defined[1].

We have systematically examined the role of INO80 during replication and found that the INO80 complex is recruited to replication origins (autonomous replicating sequences; ARSs) across the genome under replication stress. Notably, although the *ino80* mutant is hypersensitive to HU on plates[3–5], we did not identify any important role for INO80 in maintaining replication fork stability in response to HU. However, we discovered that INO80 is specifically involved in the DNA damage tolerance pathway during replication. Here, we show that in the yeast *Saccharomyces cerevisiae*, INO80 is dispensable for maintaining replication fork stability after HU treatment, but it is required for adequate processing of replication forks in MMS-treated cells through its role in the DNA damage tolerance pathway. Mechanistically, INO80 regulates ubiquitination of PCNA and Rad51-mediated processing of recombination intermediates at impeded replication forks by allowing proper recruitment of Rad18 and Rad51, factors known to be involved in fork resolution. These findings establish INO80 as a newly identified regulator of DNA damage tolerance pathways and reveal the importance of ATP-dependent chromatin remodeling in maintaining genomic integrity during DNA replication.

RESULTS

Genome-wide recruitment of INO80 to ARSs during S phase

The hypersensitivities of the *ino80* mutant to DNA replication blocking agents such as MMS and HU, together with our observation that Ino80 expression is upregulated specifically during S phase, indicate that INO80 may have a direct role in the response to stalled replication forks[5,6]. Moreover, the observation that INO80 does not have a major effect on the transcription of known genes implicated in DNA replication (**Supplementary Table 1**) led us to investigate whether INO80 directly binds ARSs. Given that INO80 was reported to localize to some ARSs in yeast[2–4], we extended our analyses to a genome-wide level by combining chromatin immunoprecipitation with high-density oligonucleotide array detection (ChIP-Chip)[9]. We engineered a Flag-tagged INO80 strain to analyze INO80 localization in cells arrested at the S phase with HU. As a control, we monitored Cdc45 binding to chromosomes to identify early-firing ARSs[9]. An example of the ChIP-Chip analysis on chromosome VI is shown in **Supplementary Figure 1**.

Our data indicate that INO80 binds 45% of known ARSs, as defined by the *Saccharomyces* Genome Database (SGD), during S phase (**Fig. 1a**). In addition, INO80 binding sites are distributed along all chromosomes (data not shown), suggesting that INO80 is an important

[1]Department of Carcinogenesis, Science Park Research Division, M.D. Anderson Cancer Center, Smithville, Texas, USA. [2]Institute of Human Genetics, CNRS UPR 1142, Montpellier, France. [3]Gene Research Center, Tokyo Institute of Technology, Midori-ku, Yokohama, Japan. [4]Department of Pathology, Harvard Medical School, Boston, Massachusetts, USA. [5]Department of Biochemistry and Molecular Biology, Mayo Clinic College of Medicine, Rochester, Minnesota, USA. [6]Department of Molecular and Human Genetics, Baylor College of Medicine, Houston, Texas, USA. [7]These authors contributed equally. Correspondence should be addressed to X.S. (snowshen@mac.com).

Received 16 June; accepted 3 September; published online 25 October 2009; doi:10.1038/nsmb.1686

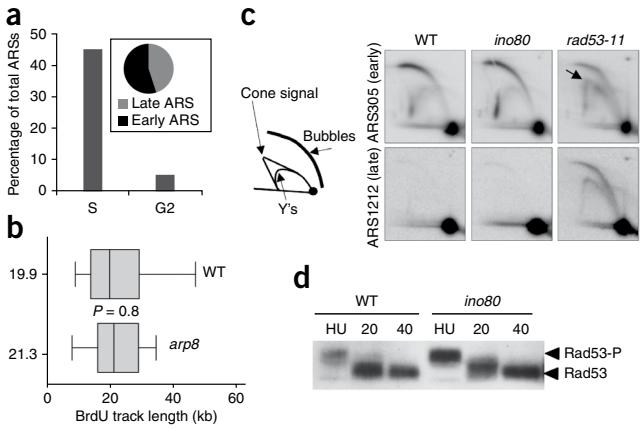

Figure 1 INO80 is dispensable for fork stabilization after HU treatment. (**a**) Genome-wide ChIP-chip analysis of Flag-INO80 binding to ARSs sequences. Cells were synchronized in G1 with α-factor for 2 h and released into S phase in the presence of 200 mM HU (Sigma) for 60 min, or arrested in G2/M by incubating logarithmically growing cultures for 2.5 h in YPD medium with benomyl (Sigma, 80 μg ml^{-1}). Cell arrest was checked microscopically and by FACS. Yeast ARSs sequences were identified from SGD, and INO80 binding to ARSs was expressed as percentage of total genome ARSs and classified as early- and late-firing origins. The analysis was obtained from multiple ChIP-chip datasets. (**b**) DNA combing analysis of replication fork progression in unchallenged forks. Asynchronous wild-type and *arp8* cells were incubated with BrdU for 40 min. The DNA fibers were stretched on silanized coverslips and visualized by microscopy. The distribution of BrdU track length in wild-type and *arp8* cells is represented. Boxes, 25–75 percentile range; whiskers, 10–90 percentile range; vertical bars, medians. *P* values: Mann-Whitney rank-sum test. (**c**) 2D gel analysis of DNA intermediates derived from replication fork collapse. Early-log-phase cultures of wild-type (WT), *ino80* and *rad53-11* cells were arrested in G1 by incubation with α-factor for 2.5 h and released into S phase in the presence of 200 mM HU. Cells were harvested after 90 min, and replication intermediates at the early origin *ARS305* and the late origin *ARS1212* were analyzed by 2D gels[16]. A schematic representation of replication intermediates is presented. Arrows mark intermediates derived from fork collapse. (**d**) Detection of phosphorylated Rad53 by western blot. Wild-type (WT) and *ino80* cultures synchronized in G1 with α-factor for 2.5 h were released into S phase in medium containing 200 mM HU for 1 h. Next, cells were released from the HU block by resuspension in YEPD medium, and samples were taken at the indicated times. Rad53 phosphorylation was detected using an anti-Rad53 (SC6749, Santa Cruz). Rad53-P, phosphorylated form of Rad53.

factor during replication across the genome. Furthermore, ChIP-Chip analysis of G2 arrested cells (**Fig. 1a**) shows that INO80 binds only 4% of total ARSs (INO80 expression in G2 and S phase are similar; data not shown), indicating that INO80 binding of ARSs is S-phase specific. Analysis of microarray data originated from S-phase–synchronized, MMS-treated *ino80* cells (**Supplementary Table 1**) indicates that only 6.5% of the INO80 binding signal at ARSs correlate with promoter regions of genes regulated by INO80. By contrast, 45% of INO80 binding signal at promoter regions concur with INO80-regulated genes (see Online Methods for details), suggesting that INO80 activities at ARSs are not related to transcription. Finally, we noticed that INO80 binds both early and late ARSs, with a slight preference for early ARSs (**Fig. 1a**), indicating that INO80 is broadly required by both early and late ARSs. Together, these findings establish that INO80 is specifically and globally recruited to ARSs during S phase and that the presence of INO80 at ARSs is associated with a replication-related activity.

INO80 is dispensable for replication fork progression

We first examined whether INO80 is necessary for replication fork movement in unperturbed normal replication using DNA combing analysis, which allows direct visualization of single DNA fibers[10]. Notably, DNA combing requires a strain constructed in a W303 genetic background that efficiently incorporates bromodeoxyuridine (BrdU). However, *INO80* is essential in the W303 background (unpublished observations), so we performed DNA combing using the *arp8* mutant instead. Arp8 is an INO80-specific subunit that is required for INO80 ATPase activity, such that the loss of Arp8 mimics the loss of INO80[11].

Wild-type and *arp8* cultures were incubated in the presence of BrdU to stain newly replicating DNA. DNA was then isolated in plugs and stained with an antibody to BrdU (anti-BrdU)[12], and the DNA fibers were quantified under the microscope. Notably, we did not observe any significant difference in BrdU track lengths between wild-type and *arp8* cells, indicating that INO80 is dispensable for fork progression during unperturbed replication (**Fig. 1b**). However, given that *ino80* cells are hypersensitive to HU in plates[3–6], we investigated whether INO80 is required for fork progression under HU-induced replication stress.

INO80 is dispensable for replication after HU treatment

In the presence of HU, the Rad53-dependent intra-S checkpoint is activated through Rad53 phosphorylation[13–15]. In the absence of Rad53, HU-stalled replication forks collapse and the repression of late firing origins is lost[16]. As the *ino80* mutant is hypersensitive to HU, we investigated whether INO80 is required for fork stability.

Wild-type and *ino80* cultures were synchronized in G1 and released into S phase in medium containing 0.2 M HU to arrest replication forks in early S phase. The DNA was then extracted for two-dimensional (2D) gel analysis of ARS305 and ARS1212 (**Fig. 1c**). As indicated by the arc representing replication fork progression (bubbles), origins were properly fired in both wild-type and *ino80* cells. Moreover, HU induced a reversible fork arrest in wild-type cells following G1 release as previously described[16], with no signs of fork collapse (ARS305 in **Fig. 1c**). Unlike the *rad53* mutant, *ino80* mutant cells were proficient not only in the maintenance of HU-arrested forks, but also in the repression of late-firing origins represented by ARS1212 (fork collapse is marked by the presence of a cone signal in **Fig. 1c**). Moreover, this effect is global, as we did not observe any difference between wild-type and *ino80* cells in the activation of the phosphorylated form of γ-H2AX (a marker of DSB formation[17]) or the phosphorylated form of Rad53 (a checkpoint activation marker[16]) during HU arrest or recovery (**Fig. 1d**). FACS analysis indicated that INO80 is not required for the recovery of replication upon the removal of HU (data not shown). Together, our results suggest that the HU hypersensitivity of the *ino80* mutant is not directly related to a defect in replication fork stability or recovery under acute HU-induced replication stress. However, recent studies indicate that mutants of several genes encoding factors involved in the DNA damage tolerance pathways, such as *Sgs1* and *Rtt101*, show no defects in fork stability and recovery after HU treatment when assessed by 2D electrophoresis and pulsed-field gel electrophoresis (PFGE), despite being hypersensitive to HU in plates[18,19]. As this phenotype resembles the *ino80* phenotype, we hypothesized a link between INO80 and the DNA damage tolerance pathway.

INO80 is required to process MMS-stalled replication forks

In *S. cerevisiae*, bypass of MMS-induced lesions during S phase is mediated by activation of the *RAD6*-mediated DNA damage tolerance

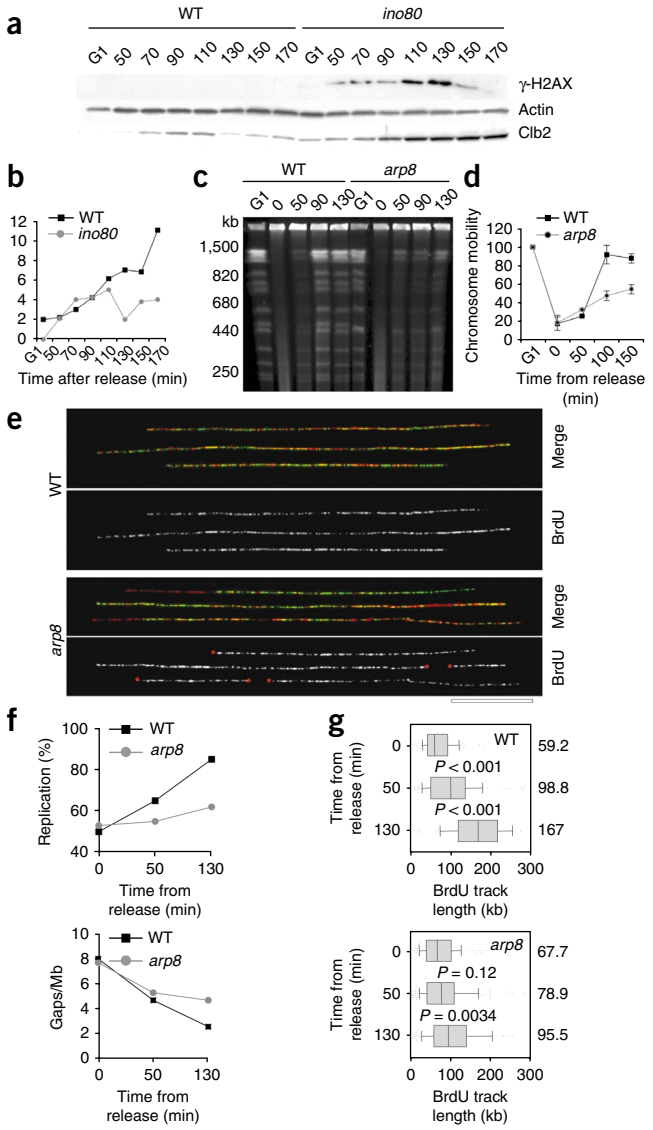

Figure 2 INO80 is required to restart MMS-stalled replication forks. (**a**,**b**) Detection of γ-H2AX by western blot. Exponentially growing wild-type (WT) and *ino80* cultures (25 °C) were arrested in G1 with α-factor for 2.5 h and treated with 0.02% MMS for 30 min before release into S phase. Cells were released from G1 block in fresh medium, and samples were taken at the indicated times for western blotting. Western blots showing γ-H2AX, Clb2 and actin (loading control) are presented in **a**, and quantification of Clb2 signal as an indicator of cell cycle progression in **b**. (**c**–**g**) PFGE and DNA combing analysis of replication fork restart after MMS treatment. Wild-type (PP633) and *arp8* (PP829) cultures were grown at 25 °C in complete synthetic medium and synchronized in G1 using 2 μg ml^{-1} α-factor for 2.5 h. Cells were released from G1 block by filtration and arrested in early S phase with 0.033% methylmethane sulfonate (Sigma). After 60 min, MMS was quenched for 5 min using 2.5% sodium thiosulfate, and cells were resuspended in fresh medium. Samples for PFGE and DNA combing were collected at the indicated times after release. (**c**) PFGE analysis of S-phase completion after MMS. (**d**) Quantification of chromosome mobility calculated for eight representative chromosomes. (**e**) DNA combing analysis of replication fork recovery after MMS. DNA fibers stretched on silanized coverslips were visualized with antibodies against BrdU (green) and ssDNA (red). Representative fibers from wild-type and *arp8* cells were collected 130 min after release from MMS. Red asterisks, stalled forks. Bar, 50 kb. (**f**) For each time point, the percentage of replication and the number of unreplicated gaps were determined in wild-type and *arp8* cells. (**g**) Distribution of BrdU track length in wild-type and *arp8* cells. Boxes, 25–75 percentile range; whiskers, 10–90 percentile range; vertical bars, medians. *P* values: Mann-Whitney rank-sum test.

pathway[20–23], and mutants of genes involved in this pathway are hypersensitive to MMS[24]. Thus, the MMS hypersensitivity of the *ino80* mutant[5] led us to examine formation of γ-H2AX as a marker of double strand breaks (DSBs) that might result from improper processing of obstructed replication forks[17]. We found that *ino80* mutant cells that were synchronized in G1 and treated with MMS before release into S phase accumulated γ-H2AX only when cells were allowed to progress through the S phase (**Fig. 2a**). By contrast, cells treated with MMS in G1 that were not released into the S phase did not accumulate γ-H2AX (**Supplementary Fig. 2a**), indicating that this effect is S-phase specific. Furthermore, the accumulation of Clb2, a G2 cyclin, in the *ino80* mutant indicates a delay at the G2 checkpoint due to generation of DSBs during S phase[25] (**Fig. 2b**). These results suggest that INO80 is necessary during DNA replication to avoid DSB generation as a consequence of improper processing of impeded replication forks.

INO80 is required to restart MMS-stalled forks

To further investigate whether the accumulation of γ-H2AX in the *ino80* mutant is related to deficient replication fork activities, we examined replication fork recovery and progression using PFGE and DNA combing[12] (**Fig. 2c–g**). Wild-type and *arp8* cultures released from G1 synchronization were treated with MMS in S phase. MMS was then inactivated and cells were allowed to finish replication.

PFGE analysis showed that, unlike the *arp8* mutant, wild-type cells completed S phase within 90 min of MMS inactivation (**Fig. 2c**,**d**). Moreover, examination of specific chromosomes by Southern hybridization further confirmed the recovery defects observed in the *arp8* mutant (**Supplementary Fig. 2d**). Consistent with a defect in replication recovery, *arp8* mutant cells were arrested in S phase (**Supplementary Fig. 2b**) and their viability was reduced after MMS treatment (**Supplementary Fig. 2c**). Moreover, the marked reduction in the length of BrdU tracks (**Fig. 2g**,**e** and **Supplementary Fig. 2e**), together with the persistence of unreplicated gaps observed in the *arp8* mutant by combing analysis (**Fig. 2f**,**e** and **Supplementary Fig. 2e**), suggest that there is a defect in fork recovery. Combined, these results establish that INO80 is required to efficiently restart MMS-stalled replication forks and suggest that INO80 is necessary for proper processing of stalled replication forks after MMS treatment.

INO80 remodeling activity affects PCNA ubiquitination

Given that MMS sensitivity, as well as the inability to resume replication fork movement after MMS treatment in the *ino80* mutant, resembles the phenotype of null mutants of genes involved in the DNA damage tolerance pathway[21], we investigated whether INO80 might be necessary for activation of the primary step in this pathway, PCNA ubiquitination. After MMS treatment, PCNA is either mono- or polyubiquitinated at its K164 residue, leading to fork resolution through the error-prone and error-free pathways, respectively[20]. More importantly, a point mutant with a substitution in Lys164 that renders the protein deficient in PCNA ubiquitination (K164R) is also sensitive to MMS[26].

To analyze PCNA ubiquitination, wild-type and *ino80* cultures were synchronized in G1 and released into S phase in medium containing MMS. Proteins were then extracted in trichloroacetic acid, and PCNA was pulled down under denaturing conditions using anti-PCNA[20,27]. The ubiquitinated forms of PCNA, although low in abundance, were identified with anti-ubiquitin[20]

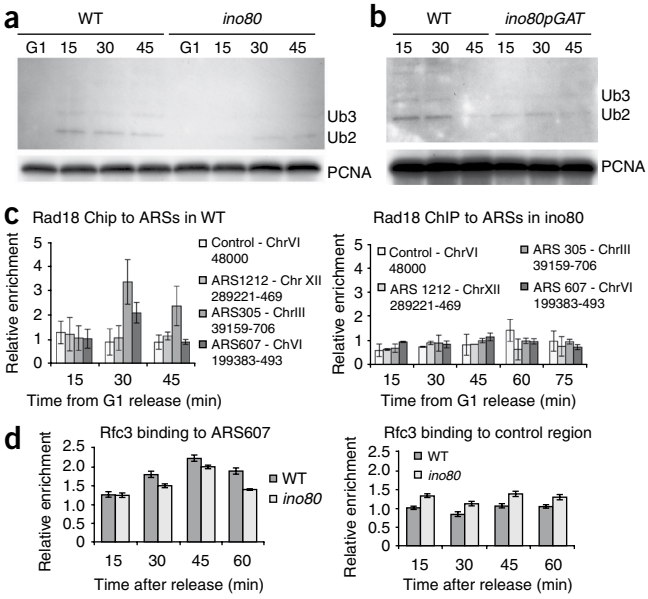

Figure 3 INO80 is involved in the DNA damage tolerance pathway. (**a**,**b**) Western blot analysis of PCNA ubiquitination. Cells were synchronized in G1 with α-factor for 2.5 h and released into S phase in medium with 0.02% MMS. Proteins were extracted by TCA precipitation[27] (see Online Methods), and PCNA was immunoprecipitated under denaturing conditions and detected by western blot with the same antibody. The ubiquitinated forms of PCNA were identified with a commercially available anti-ubiquitin antibody. Ub2 and Ub3 represent the ubiquitinated forms of PCNA. PCNA ubiquitination is shown in wild type (WT) and *ino80* mutants (**a**) as well as in an ATPase-deficient mutant (*ino80pGAT*; **b**). (**c**) ChIP analysis of Rad18 recruitment to ARSs during S phase. Wild-type and *ino80* cells were tagged with Flag at the *RAD18* locus, synchronized in G1, treated with 0.02% MMS in G1, and then released into S phase in medium containing 100 mM HU and 0.02% MMS. ChIP analyses were performed at the indicated ARSs. Data analyzed from three independent experiments; error bars indicate s.d. (**d**) Rfc3 recruitment to ARS607 during S phase. Rfc3 binding to ARS 607 was analyzed in wild-type and *ino80* cells as described in **c**. DNA was cross-linked at the indicated times for ChIP analysis, and Rfc3 was immunoprecipitated with am Rfc3-specific antibody (see Online Methods). Primers used correspond to ARS607 and a control non-ARS sequence in chromosome VI. Data analyzed from three independent experiments; error bars indicate s.d.

(**Fig. 3a**). We reproducibly observed that the ubiquitinated forms of PCNA were delayed in induction and moderately but consistently reduced in abundance in the *ino80* mutant, whereas expression of the unmodified form of PCNA was not affected. To confirm the identity of the PCNA ubiquitinated bands, we performed the same pulldown analysis using a *pcna K164R* mutant that cannot be ubiquitinated after MMS treatment[26]; the PCNA ubiquitinated bands were absent in this strain (**Supplementary Fig. 3a**). These results indicate that INO80 is necessary for efficient PCNA ubiquitination during replication stress.

The observation that a point mutation (leading to a K737A substitution) that specifically abolishes the ATPase activity of INO80 is also hypersensitive to MMS[5] led us to investigate whether INO80 chromatin remodeling activity is required for PCNA ubiquitination. Similar to the *ino80* null mutant, the *ino80* point mutant strain (*K737A*) showed reduced PCNA ubiquitination in the same assays (**Fig. 3b**). To determine whether the delay in PCNA ubiquitination is a consequence of a delay in entering S phase in the *ino80* mutant cells, we monitored the acetylation of histone H3 at lysine 56 (H3K56)[28], which is specifically modified during S phase and required for replisome stability, as well as the expression of Clb2, another S-phase marker. Both H3 K56 acetylation and Clb2 were induced normally in the *ino80* mutant under the same experimental conditions[28], indicating that *ino80* mutant cells enter the S phase without delay (**Supplementary Fig. 3b**).

To confirm that the delayed and inefficient PCNA ubiquitination is not an artifact of a delay in entering the S phase in the *ino80* mutant, we analyzed PCNA ubiquitination in whole-cell extracts of asynchronous cultures, in which the percentage of S-phase cells is similar in wild-type cells and *ino80* mutants. As described, the diubiquitinated form of PCNA increases after MMS treatment in the wild type, but is reduced in both the *rad6* and *rad5* mutants[20]. Consistent with the PCNA pulldown experiments, we also observed that PCNA ubiquitination was reduced in the *ino80* mutant, whereas both the sumoylated and unmodified forms of PCNA were unaffected (**Supplementary Fig. 3c**). Similarly, the INO80 ATPase point mutant (*K737A*) was also defective in PCNA ubiquitination (**Supplementary Fig. 3d**). Together, these data indicate that INO80 and its chromatin remodeling activities are important for efficient PCNA ubiquitination after MMS-induced replication stress.

INO80 is necessary to recruit Rad18 to replication forks

The defect in PCNA ubiquitination in the *ino80* mutant led us to investigate whether INO80 is necessary to allow recruitment of PCNA ubiquitinating proteins to replication forks. As the first protein known to be recruited to stalled replication forks induced by MMS is the E3 ligase Rad18 (ref. 20), we used ChIP to investigate whether INO80 is necessary for Rad18 recruitment to ARSs (**Fig. 3c**). Notably, INO80 does not affect the expression of genes involved in the damage tolerance pathway when assessed by genome-wide microarray transcription analysis in MMS-treated, S-phase–synchronized cells (**Supplementary Table 1**).

Cells tagged at the *RAD18* locus were synchronized in G1 and treated with MMS before release into the S phase. Next, cultures were released into the S phase and fork movement was slowed by addition of HU (100 mM) as described[23]. Our ChIP analysis indicated that, unlike wild-type cells, in which Rad18 signal was enriched at multiple early ARSs (ARS607 and ARS305), Rad18 recruitment is not detectable in the *ino80* mutant (**Fig. 3c**). Furthermore, there was no significant binding signal at a late ARS (ARS 1212) in either the wild type or the *ino80* mutant.

As the defect in Rad18 recruitment could be due to either delayed or unsynchronized replication in the *ino80* mutant, we performed the same ChIP analysis using Rfc3, a bona fide replisome component, and found that the Rfc3 binding profile was similar in the wild type and the *ino80* mutant (**Fig. 3d**). Next, we monitored the progression of S phase using FACS analysis to show that both wild-type and *ino80* mutant cells progress through S phase with synchrony (**Supplementary Fig. 3e**). Notably, a control primer on chromosome VI indicates that both Rad18 and Rfc3 binding are specific to the ARS sequences (**Fig. 3c**,**d**). Finally, the ARS selection for ChIP assays was based on our ChIP-Chip whole genome analysis, and both ARS305 and ARS607 are INO80-binding ARSs, whereas ARS1212 is not. These analyses further establish that even though the normal loading of the replisome is not affected, there is a specific defect in Rad18 recruitment to ARSs in the *ino80* mutant. Together, our results indicate that INO80 is required to efficiently recruit Rad18, which initiates the PCNA ubiquitination pathways.

INO80 affects Rad51-dependent recombination

Recent findings suggest that both the *RAD6* and *RAD51* pathways promote resolution of replication blocks in yeast[29]. Moreover,

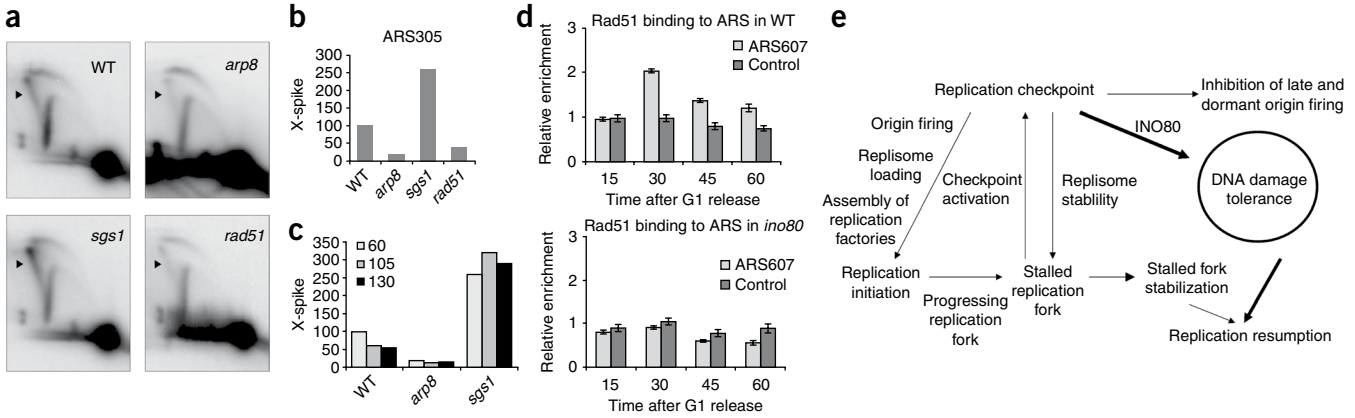

Figure 4 INO80 is required for Rad51-dependent recombination intermediates formation after MMS treatment. (**a**–**c**) Wild-type (PP633), *arp8* (PP829), *sgs1* (PP118) and *rad51* (PP484) cultures were arrested for 2.5 h in G1 with α-factor and released into S phase in the presence of 0.1% MMS. (**a**) 2D gel analysis of an EcoRI fragment encompassing the early origin ARS305. Arrowhead, X-spikes indicating joined molecules. (**b**) Relative number of X-spikes in wild-type (WT), *arp8, sgs1* and *rad51* cells after 60 min of MMS treatment. (**c**) Variation of X-spike intensity over time in the presence of MMS. (**d**) ChIP analysis of Rad51 recruitment to ARSs in S phase. Wild-type and *ino80* cells were synchronized in G1, treated with 0.02% MMS in G1, then released into S phase in medium containing 100 mM HU and 0.02% MMS. Rad51 ChIP was performed with a specific antibody. Primers correspond to ARS607 and a control non-ARS sequence in chromosome VI. Data analyzed from three independent experiments; error bars represent s.d. (**e**) A model depicting the involvement of INO80 in DNA replication (adapted from ref. 32). Major steps and pathways of DNA replication are presented, and the main function of INO80 is highlighted in bold. A detailed model is shown in **Supplementary Figure 6**.

Rad51 recombinant activity at obstructed forks generates 'X-spike structures', joint DNA molecules that are subsequently resolved by Sgs1. These homologous recombination intermediates are intrinsically different from substrates generated after replication fork collapse or at conventional non–S-phase DSBs[30,31]. More importantly, Rad51-mediated formation of X-spike molecules at forks requires not only PCNA ubiquitination but also Rad18 activity[32]. Thus, we investigated whether INO80 is required for Rad51-mediated X-spike generation at obstructed forks (**Fig. 4**).

Our results confirmed that in the *sgs1* mutant, which lacks the helicase required to resolve joint molecules, these structures accumulate and result in enhanced X-spike intensity in 2D gels[19] (**Fig. 4a**, arrow). However, in the *rad51* and *arp8* mutants these joint molecules are markedly reduced (**Fig. 4a**,**b**). Moreover, kinetic studies indicated that the reduction of joint molecules in the *arp8* mutant is persistent and is not due to a delay in generating such molecules (**Fig. 4c** and **Supplementary Fig. 4a**). These results show that INO80 is involved in the Rad51-dependent processing of replication intermediates after MMS-induced replication block.

INO80 is necessary to recruit Rad51 to replication forks

As INO80 is necessary to recruit Rad18 to replication forks and to recruit Rad51 during conventional DSB repair[33], we examined whether recruitment of Rad51to ARSs also requires INO80. Using anti-Rad51, we performed ChIP analysis under the same experimental protocol used for Rad18 ChIP (**Fig. 4d**). As previously described[23], Rad51 is recruited to ARS607 but not to a control region in wild-type cells during S phase (**Fig. 4d**). By contrast, recruitment of Rad51 to ARS607 was significantly impaired in the *ino80* mutant (**Fig. 4d**). Furthermore, Rad51 was not recruited to several ARSs that did not show INO80 binding in our ChIP-Chip analysis (ARS501, ARS601 and ARS1212), either in wild-type or in *ino80* mutant cells (**Supplementary Fig. 4b**). These analyses show that INO80 is upstream of Rad51. Together, our results establish INO80 as a regulator of DNA damage tolerance during replication, through its ability to influence the recruitment of factors in both the *RAD6* and *RAD51* pathways.

DISCUSSION

Our systematic analysis reveals that INO80 has a specific function in DNA damage tolerance pathways rather than in fork progression or stability (**Fig. 4f**). Our model suggests that INO80 binds replication forks during S phase and allows access of proteins in the *RAD6* and *RAD51* pathways to process obstructed replication forks (**Supplementary Fig. 5**). Chromatin remodeling by INO80 facilitates the recruitment of Rad18 and Rad51 to replication forks, leading to the formation of X-spike structures, a process that requires both Rad18 activity and PCNA ubiquitination. Our study shows that the INO80 chromatin remodeling complex is a relatively early player in this pathway, thus establishing chromatin remodeling as a new regulatory event in DNA damage tolerance during replication.

Our observation that the *ino80* mutant grows slower than the wild-type strain indicates that INO80 might have a role during unperturbed DNA replication[1,11]. However, our combing analysis (**Fig. 1b**) suggests that INO80 is not necessary during unperturbed replication. Results from our study also indicate that INO80 binds not only to early- but also to late-firing origins across the genome. Although unexpected, our results confirm those of previous work[2] and raise the question of whether INO80 has similar or distinct functions at early and late firing origins.

Notably, as the *ino80* mutant is hypersensitive to HU, it is plausible that INO80 is involved in replisome stability at stalled replication forks, as previously reported[3]. However, our analysis and that of others[4] show that under HU stress replication forks do not collapse (**Fig. 1c**). In fact, we did not observe any defect in the recovery of replication upon HU removal, as reported[4]. Instead, our systematic analyses identified one major and specific role of INO80 in MMS-induced DNA damage tolerance during replication. The differential involvement of INO80 in HU and MMS responses highlights the distinctions among pathways involved in dealing with specific types of replicative stress.

The role of INO80 in damage tolerance is clearly distinct from its role in DSB repair[6,8]. As previously shown, the *nhp10* mutant is defective in DNA resection during conventional DSB repair[6], but it is not sensitive to MMS[6] or defective in fork recovery after MMS treatment as measured by PFGE (**Supplementary Fig. 6a**–**c**). In addition—and similar to the

situation with the Rtt101 complex, which is required for fork recovery after MMS but not for homologous recombination at DSBs[18,30]—Arp8, but not Nhp10, is required for recombination of stalled forks as assessed by the rate of unequal sister chromatid exchange induced by fork stalling at MMS lesions[30,34] (**Supplementary Fig. 6d**). This supports a unique role for INO80 at MMS-stalled forks. Our study has established a previously undescribed role of the INO80 complex in DNA damage tolerance pathways during DNA replication, which is distinct from its role in DSB repair.

METHODS

Methods and any associated references are available in the online version of the paper at http://www.nature.com/nsmb/.

Accession codes. GEO: MMS-treated INO80 microarray data, GSE18555; INO80 ChIP-Chip dataset, GSE18570.

Note: Supplementary information is available on the Nature Structural & Molecular Biology website.

ACKNOWLEDGMENTS

We thank E. Schwob (IGMM) and J. Rouse (MRC) for strains; H. Ulrich (Cancer UK) for strains and protocols; M.A. Osley (University of New Mexico) for protocols; P. Sung (Yale University) for Rad51 antibody; J. Delrow and R. Basom (Fred Hutchinson Cancer Research Center, FHCRC) for microarray analysis; K. Claypool and S. Hasley (M.D. Anderson Cancer Center (MDACC)) for technical assistance; and members of the Shen lab for comments on the manuscript. This work was supported by funds and grants from MDACC, ACS (RSG-05-060-01-GMC) and the National Institute of Environmental Health Sciences (ES07784) to X.S. (MDACC), from the Rosalie B. Hite Fellowship to K.B.F. (MDACC), from the Fondation Recherche Medicale, the Centre National de la Recherche Scientifique, the Agence Nationale de la Recherche and the Institut National du Cancer to P.P.; by an ARC fellowship to C.A. (CNRS); and by a grant from the US National Institutes of Health (GM71729) to Z.Z. K.S. was supported by a grant of the Cell Innovation Project and Grant-in-Aid for Scientific Research (S) from the Ministry of Education Science and Sports (MEXT), Japan. Y.K. is a Global Center of Excellence (GCOE) research associate.

AUTHOR CONTRIBUTIONS

K.B.F. and X.S. designed the study with contributions from X.H., S.W. and Y.S.; K.B.F., C.A., P.P., Y.K., K.S., J.H. and Z.Z. carried out experiments; T.W. and J.X. provided technical assistance. K.B.F. and X.S. wrote the paper.

Published online at http://www.nature.com/nsmb/.
Reprints and permissions information is available online at http://npg.nature.com/reprintsandpermissions/.

1. Falbo, K.B. & Shen, X. Chromatin remodeling in DNA replication. *J. Cell. Biochem.* **97**, 684–689 (2006).
2. Vincent, J.A., Kwong, T.J. & Tsukiyama, T. ATP-dependent chromatin remodeling shapes the DNA replication landscape. *Nat. Struct. Mol. Biol.* **15**, 477–484 (2008).
3. Papamichos-Chronakis, M. & Peterson, C.L. The Ino80 chromatin-remodeling enzyme regulates replisome function and stability. *Nat. Struct. Mol. Biol.* **15**, 338–345 (2008).
4. Shimada, K. *et al.* Ino80 chromatin remodeling complex promotes recovery of stalled replication forks. *Curr. Biol.* **18**, 566–575 (2008).
5. Shen, X., Mizuguchi, G., Hamiche, A. & Wu, C. A chromatin remodelling complex involved in transcription and DNA processing. *Nature* **406**, 541–544 (2000).
6. Morrison, A.J. *et al.* INO80 and gamma-H2AX interaction links ATP-dependent chromatin remodeling to DNA damage repair. *Cell* **119**, 767–775 (2004).
7. Morrison, A.J. *et al.* Mec1/Tel1 phosphorylation of the INO80 chromatin remodeling complex influences DNA damage checkpoint responses. *Cell* **130**, 499–511 (2007).
8. van Attikum, H., Fritsch, O., Hohn, B. & Gasser, S.M. Recruitment of the INO80 complex by H2A phosphorylation links ATP-dependent chromatin remodeling with DNA double-strand break repair. *Cell* **119**, 777–788 (2004).
9. Katou, Y. *et al.* S-phase checkpoint proteins Tof1 and Mrc1 form a stable replication-pausing complex. *Nature* **424**, 1078–1083 (2003).
10. Michalet, X. *et al.* Dynamic molecular combing: stretching the whole human genome for high-resolution studies. *Science* **277**, 1518–1523 (1997).
11. Shen, X., Ranallo, R., Choi, E. & Wu, C. Involvement of actin-related proteins in ATP-dependent chromatin remodeling. *Mol. Cell* **12**, 147–155 (2003).
12. Tourrière, H., Versini, G., Cordon-Preciado, V., Alabert, C. & Pasero, P. Mrc1 and Tof1 promote replication fork progression and recovery independently of Rad53. *Mol. Cell* **19**, 699–706 (2005).
13. Branzei, D. & Foiani, M. The Rad53 signal transduction pathway: Replication fork stabilization, DNA repair, and adaptation. *Exp. Cell Res.* **312**, 2654–2659 (2006).
14. Branzei, D. & Foiani, M. Interplay of replication checkpoints and repair proteins at stalled replication forks. *DNA Repair (Amst.)* **6**, 994–1003 (2007).
15. Branzei, D. & Foiani, M. Regulation of DNA repair throughout the cell cycle. *Nat. Rev. Mol. Cell Biol.* **9**, 297–308 (2008).
16. Lopes, M. *et al.* The DNA replication checkpoint response stabilizes stalled replication forks. *Nature* **412**, 557–561 (2001).
17. Rogakou, E.P., Pilch, D.R., Orr, A.H., Ivanova, V.S. & Bonner, W.M. DNA double-stranded breaks induce histone H2AX phosphorylation on serine 139. *J. Biol. Chem.* **273**, 5858–5868 (1998).
18. Luke, B. *et al.* The cullin Rtt101p promotes replication fork progression through damaged DNA and natural pause sites. *Curr. Biol.* **16**, 786–792 (2006).
19. Branzei, D. *et al.* Ubc9- and mms21-mediated sumoylation counteracts recombinogenic events at damaged replication forks. *Cell* **127**, 509–522 (2006).
20. Hoege, C., Pfander, B., Moldovan, G.L., Pyrowolakis, G. & Jentsch, S. RAD6-dependent DNA repair is linked to modification of PCNA by ubiquitin and SUMO. *Nature* **419**, 135–141 (2002).
21. Ulrich, H.D. Conservation of DNA damage tolerance pathways from yeast to humans. *Biochem. Soc. Trans.* **35**, 1334–1337 (2007).
22. Papouli, E. *et al.* Crosstalk between SUMO and ubiquitin on PCNA is mediated by recruitment of the helicase Srs2p. *Mol. Cell* **19**, 123–133 (2005).
23. Watts, F.Z. Sumoylation of PCNA: Wrestling with recombination at stalled replication forks. *DNA Repair (Amst.)* **5**, 399–403 (2006).
24. Chang, M., Bellaoui, M., Boone, C. & Brown, G.W. A genome-wide screen for methyl methanesulfonate-sensitive mutants reveals genes required for S phase progression in the presence of DNA damage. *Proc. Natl. Acad. Sci. USA* **99**, 16934–16939 (2002).
25. Veis, J., Klug, H., Koranda, M. & Ammerer, G. Activation of the G2/M-specific gene CLB2 requires multiple cell cycle signals. *Mol. Cell. Biol.* **27**, 8364–8373 (2007).
26. Stelter, P. & Ulrich, H.D. Control of spontaneous and damage-induced mutagenesis by SUMO and ubiquitin conjugation. *Nature* **425**, 188–191 (2003).
27. Kao, C.F. & Osley, M.A. In vivo assays to study histone ubiquitylation. *Methods* **31**, 59–66 (2003).
28. Han, J., Zhou, H., Li, Z., Xu, R.M. & Zhang, Z. Acetylation of lysine 56 of histone H3 catalyzed by RTT109 and regulated by ASF1 is required for replisome integrity. *J. Biol. Chem.* **282**, 28587–28596 (2007).
29. Gangavarapu, V., Prakash, S. & Prakash, L. Requirement of RAD52 group genes for postreplication repair of UV-damaged DNA in *Saccharomyces cerevisiae*. *Mol. Cell. Biol.* **27**, 7758–7764 (2007).
30. Duro, E., Vaisica, J.A., Brown, G.W. & Rouse, J. Budding yeast Mms22 and Mms1 regulate homologous recombination induced by replisome blockage. *DNA Repair (Amst.)* **7**, 811–818 (2008).
31. Li, X. & Heyer, W.D. Homologous recombination in DNA repair and DNA damage tolerance. *Cell Res.* **18**, 99–113 (2008).
32. Branzei, D., Vanoli, F. & Foiani, M. SUMOylation regulates Rad18-mediated template switch. *Nature* **456**, 915–920 (2008).
33. Tsukuda, T., Fleming, A.B., Nickoloff, J.A. & Osley, M.A. Chromatin remodelling at a DNA double-strand break site in *Saccharomyces cerevisiae*. *Nature* **438**, 379–383 (2005).
34. Fasullo, M., Giallanza, P., Dong, Z., Cera, C. & Bennett, T. *Saccharomyces cerevisiae* rad51 mutants are defective in DNA damage-associated sister chromatid exchanges but exhibit increased rates of homology-directed translocations. *Genetics* **158**, 959–972 (2001).

ONLINE METHODS

Strains. All strains are in S288C genetic background, except the *arp8* mutant used for DNA combing (**Supplementary Table 2**). We used standard yeast genetic techniques to create gene deletions and epitope-tagged strains.

Cell cycle and FACS analysis. We arrested cells in G1 by adding 2 μg ml^{-1} α-factor to the medium twice for 1 h per treatment. Next, we released the cultures from G1 arrest by washing in 10 mg ml^{-1} pronase and resuspension in YEPD media. For FACS analysis, we treated the cells with RNase A and proteinase K before staining with SYTOX (Invitrogen). We analyzed the cells using standard flow cytometry techniques.

PFGE analysis. DNA was run in a PFGE gel stained with ethidium bromide (Sigma) and transferred on HyBond-XL membranes (Amersham GE Healthcare) to analyze specific chromosomes by Southern blot. We quantified chromosome mobility with a Typhoon Trio+ (Amersham GE Healthcare) and determined cell viability by plating 100 cells on YPD plates after acute exposure to MMS (0.033%, 60 min). To monitor S-phase progression, we used flow cytometry (FACScalibur, Becton Dickinson) or PFGE (Gene Navigator system; Amersham GE Healthcare).

DNA combing. BrdU labeling of yeast chromosomes and DNA combing were performed as described[10,12]. Briefly, we stained the DNA with BrdU (400 μg ml^{-1}, Sigma) for 20 min before release into S phase. Next, we extracted the genomic DNA in LMP agarose plugs to a final concentration of 800 ng per plug, and we stained the DNA with YOYO-1 (Molecular Probes). We resuspended the molten DNA plugs in 5 ml of 50 mM MES buffer, pH 5.7 (Sigma), to a final concentration of 150 ng ml^{-1}. After transferring the DNA solution to a Teflon reservoir, we stretched the DNA fibers on silanized coverslips, cross-linked the DNA fibers to coverslips by baking for 2 h at 60 °C, and finally denatured the DNA molecules for 25 min in 1M NaOH. To detect BrdU we used a rat monoclonal antibody (clone BU1/75, AbCys) and a secondary antibody coupled to Alexa 488 (Molecular Probes). To visualize the DNA fibers we used a mouse antibody to ssDNA (Chemicon) and a secondary antibody coupled to Alexa 546 (Molecular Probes). We recorded and processed the images with a DM6000B microscope (Leica) equipped with a CoolSNAP HQ CCD camera (Roper Scientific) as described[35]. We measured the BrdU tracks and DNA fibers with MetaMorph v7.1 (Roper Scientific), and we performed the statistical analysis with Prism 4, GraphPad Software, Inc. (over 50 Mb of genomic DNA were analyzed).

Chromatin immunoprecipitation. *In vivo* chromatin binding assays were performed as described (http://www.epigenome-noe.net/researchtools/pdfs/p27.pdf), with the exception that anti-Flag agarose beads (Sigma) were used for INO80 immunoprecipitation, and DNA purification was performed using a PCR purification kit from Qiagen. We quantified the amplified DNA regions by real-time PCR using the MyiQ single color detection system and software from Bio-Rad and the iQ SYBR Green Super Mix (Bio-Rad). Primers used correspond to different regions on the *S. cerevisiae* genome, and their sequences are available upon request. Agarose beads coupled to a monoclonal antibody against Flag epitope, Rad51 or Rfc3 were used for immunoprecipitation. Beads without antibodies were used for background controls. ChIP data are averaged over three independent experiments with Real-time PCR performed in triplicates (s.d. shown by error bars), and quantification was performed as described[36].

ChIP-Chip analysis. ChIP and hybridization were carried out as described[9], using a *S. cerevisiae* Tiling 1.0 F Array P/N520286 from Affymetrix. Fold change value, change *P* value and detection *P* value for each locus were obtained by primary analysis (software is available on request). We used the following criteria for the discrimination of positive and negative binding signal. First, the reliability of the signal strength was judged by the detection *P* value of each locus ($P \leq 0.001$ for whole genome array). Second, the reliability of the binding ratio was judged by the change *P* value ($P \leq 0.001$ for whole genome array). Third, clusters consisting of at least 400 bp contiguous loci that satisfied the above two criteria were selected. Cdc45 binding ARSs were judged as early firing. ARSs information was downloaded from the Saccharomyces Genome Database (http://www.yeastgenome.org/). ChIP DNA was purified, amplified by random priming, digested, end-labeled with biotin-N-dATP and hybridized with Affymetrix arrays. We used custom software (T. Itoh) to determine INO80 binding sites[9], and we obtained the protein binding profile by comparison analysis of the ChIP fraction with the WCE (whole cell extract) fraction. To generate a change *P* value, we performed statistical analysis using Wilcoxon's signed-rank test, and we used a second algorithm to produce a quantitative estimate of the relative change in amount of DNA for each locus in the form of signal log ratio.

Unequal sister-chromatid exchange (uSCE) assay. uSCE was measured as described[34]. In brief, we exposed mid-log-phase cultures to 0.02% MMS for 45 min. Next we plated 2×10^6 cells on SC –histidine agar and 200 cells on YPAD. After 3 d of incubation at 30 °C, we counted the colonies and quantified the frequency of uSCE as the number of histidine-positive (His$^+$) colonies per YEPD colony-forming unit. His$^+$ recombinants are formed as a result of unequal sister-chromatid exchange involving two truncated HIS fragments at the TRP1 locus. Relative units represent the number of His$^+$ colonies per 200 YPAD colonies. Values represent the average from three independent experiments.

PCNA immunoprecipitation and ubiquitin detection. We resuspended the cell pellets in 20% TCA and lysed the cells by vortexing with glass beads[27]. After 15 min of incubation on ice, we collected the precipitated proteins by centrifugation at 18,000*g* for 15 min at 4 °C. After resuspending the protein pellet in 1× Laemmli sample buffer, we boiled and clarified the suspension by centrifugation. Next, we diluted the supernatant containing the proteins five times in IP buffer (500 mM Tris, pH 7.4, 150 mM NaCl, 0.5% Nonidet P-40) and pulled down PCNA under denaturing conditions using a specific antibody to PCNA (Z.Z.). Finally, we identified the ubiquitinated forms of PCNA using a commercially available anti-ubiquitin (Santa Cruz)[20].

35. Pasero, P., Bensimon, A. & Schwob, E. Single-molecule analysis reveals clustering and epigenetic regulation of replication origins at the yeast rDNA locus. *Genes Dev.* **16**, 2479–2484 (2002).
36. Cobb, J.A., Bjergbaek, L., Shimada, K., Frei, C. & Gasser, S.M. DNA polymerase stabilization at stalled replication forks requires Mec1 and the RecQ helicase Sgs1. *EMBO J.* **22**, 4325–4336 (2003).